Pearl-Necklace Structures in Core−Shell Molecular Brushes: Experiments, Monte Carlo Simulations, and Self-Consistent Field Modeling

Alexey Polotsky,[†,§] Marat Charlaganov,[‡,§] Youyong Xu,[||] Frans A. M. Leermakers,[‡] Mohamed Daoud,[†] Axel H. E. Müller,[||] Tomonori Dotera,[⊥] and Oleg Borisov*[,§,#]

CEA DSM-DRECAM-SPEC, F-91191 Gif-sur-Yvette Cedex, France, Laboratory of Physical Chemistry and Colloid Science, Wageningen University, NL-67003 HB Wageningen, The Netherlands, Institute of Macromolecular Compounds, Russian Academy of Sciences, 199004 St.Petersburg, Russia, Makromolekulare Chemie II, Universität Bayreuth, D-95440 Bayreuth, Germany, Department of Polymer Chemistry, Kyoto University, Katsura, Nishikyo-ku, Kyoto 615-8510, Japan, and Institut Pluridisciplinaire de Recherche sur l'Environnement et les Materiaux, F-64053 Pau Cedex, France.

Received January 17, 2008; Revised Manuscript Received March 7, 2008

ABSTRACT: We present theoretical arguments and experimental evidence for a longitudinal instability in core−shell cylindrical polymer brushes with a solvophobic inner (core) block and a solvophilic outer (shell) block in selective solvents. The two-gradient self-consistent field Scheutjens−Fleer (SCF-SF) approach and Monte Carlo (MC) simulations are employed to study a conformational transition which occurs upon a decrease in the solvent strength for the inner block from Θ to poor solvent conditions. It is found that a decrease in the solvent strength for the core block leads to an instability in the cylindrically uniform structure and the appearance of longitudinal undulations in the collapsed core of the molecular brush. This result of our modeling is in excellent agreement with experimental observations on core−shell brushes with poly(acrylic acid) (PAA) core and poly(*n*-butyl acrylate) shell, where the core forms pearl-necklace-like structures due to either a bad solvent for PAA or complexation with multivalent ions.

1. Introduction

Recent advances in synthetic polymer chemistry have made it possible to produce macromolecules of complex and well-defined topology with precise control of molecular parameters. In particular, molecular brushes i.e. polymer chains, densely grafted with multiple side chains, have attracted considerable interest, due to their extended, concentration-dependent main-chain conformation ("bottlebrushes") and supersoft rheological behavior.[1] When the side chains are block copolymers, this leads to core−shell cylindrical structures, which have been used as nanoreactors for the synthesis of nanowires[2] or anisometric nanomagnets[3] and may also have potential applications in biomedicine, e.g., as drug carriers. In the formation of nanowires and nanomagnets in the core, a peculiar phenomenon was observed. Brushes with a core of poly(acrylic acid) (PAA) and a shell of poly(*n*-butyl acrylate) (PnBA) in the mixed solvent methanol/chloroform were loaded with Cd^{2+} or Fe^{3+} ions, leading to so-called polychelates in the core of the brushes. Subsequently, the ions were converted to CdS and γ-Fe_2O_3 nanoparticles, respectively. In the polychelate state, we observed a peculiar longitudinal instability in the form of the pearl-necklace structure, which disappeared after the conversion of the metal ions to nanoparticles. This led to the assumption that the interaction of the PAA chains in the core with the multivalent counterions leads to a decrease of their solubility, which in turn might affect the structure of the bottlebrushes. Thus, we became interested in studying the conformation of the pure molecular brushes in selective solvents.

In selective solvents either the core- or the shell-forming block may collapse whereas the other block remains soluble. Core−shell molecular brushes with collapsed core and soluble corona blocks can be regarded as unimolecular micelles. In principle, such structures can be generated by self-assembly of homologous diblock copolymer in solution, but for thermodynamic reasons only in a small window of block compositions. In amphiphilic core−shell brushes one can independently tune the solubility of the core- and shell-forming blocks, e.g., by varying solvent composition, temperature, salinity, or pH in the solution. Hence, by incorporating temperature- or pH-sensitive building blocks one can accomplish core−shell brushes with stimuli-responsive features which are most attractive for a number of potential applications. Here we focus on systems without ionic interactions, while results on polyelectrolyte core−shell brushes will be presented elsewhere.

Conformations of molecular brushes with nonionic homopolymer side chains have been studied on the basis of scaling[4−7] and mean-field[8,9] theories. Theory[8,9] predicts that a molecular brush collapsed under poor solvent strength conditions keeps its uniform cylindrical shape beyond a certain solvent strength threshold. Further decrease in the solvent strength provokes a longitudinal instability in the cylindrically uniform structure of the collapsed brush.[9] However, the collapse transition in homopolymer molecular brushes can be hardly observed experimentally due to their aggregation, except for extremely dilute solutions.

On the contrary, core−shell brushes with collapsed core blocks and soluble terminal blocks are stabilized with respect to aggregation due to repulsion between the shells. Therefore, conformations of the core−shell brushes in selective solvents can be studied by multiple experimental solution techniques, including neutron and X-ray scattering and particularly cryo-TEM, but also deposited on surfaces, e.g., by AFM.[1] As we demonstrate below, cryo-TEM and AFM images provide clear indication that cylindrical unimolecular micelles formed in the

* To whom correspondence should be addressed.
[†] CEA DSM-DRECAM-SPEC.
[§] Institute of Macromolecular Compounds, Russian Academy of Sciences.
[‡] Laboratory of Physical Chemistry and Colloid Science, Wageningen University.
[||] Makromolekulare Chemie II, Universität Bayreuth.
[⊥] Department of Polymer Chemistry, Kyoto University.
[#] Institut Pluridisciplinaire de Recherche sur l'Environnement et les Materiaux.

10.1021/ma800125q CCC: $40.75
Published on Web 05/10/2008

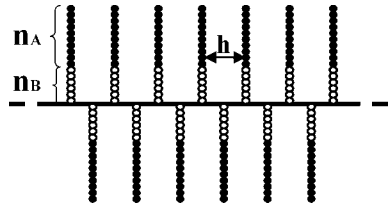

Figure 1. Schematic presentation of a core−shell molecular bottle brush: n_B and n_A are the numbers of monomer units in the core (B) and in the shell (A) blocks of a grafted chain, respectively; h is the axial separation between grafting points.

core−shell copolymer brushes with soluble shell block A and poorly soluble core block B may exhibit a longitudinal instability and split up into a necklace structure with collapsed B domains of finite size decorated by soluble coronas of terminal A blocks.

The aim of the present study is to apply a combination of the numerical self-consistent field Scheutjens−Fleer (SCF-SF) method in its two gradient version and the Monte Carlo (MC) technique for the analysis of the conformational transition occurring in core−shell molecular brushes upon a decrease in the solvent strength for the core-forming block below the Θ-point. The results of the modeling are applied to rationalize the experimental observations of pearl-necklace structures of PAA-*b*-PnBA brushes in the presence of Cd^{2+} or Fe^{3+} ions.[2,3] The advantage of the SCF-SF method over analytical theoretical approaches is the ability to avoid most of approximations except of the mean-field one. In particular, it enables to carefully explore the conformational transition related to the collapse of the inner block and to analyze the dependence of the structural properties of the brush in a wide range of molecular architecture parameters, i.e., degree of polymerization and grafting density. The precision in calculation of equilibrium properties of the system achieved by SCF-SF approach is almost the same as in MC or molecular dynamics (MD) techniques, but the efficiency of calculations is orders of magnitude higher. On the contrary, the advantage of the MC approach is that it enables to avoid the local cylindrical approximation used in SCF calculations and account explicitly for the flexibility of the main chain. Both computational methods enable us to visualize conformational changes both in the core and in the corona of the core−shell brush upon variation of the solvent strength for the core blocks.

The paper is organized as follows: In section 2, we present theoretical considerations on the collapse transition in molecular brushes. In section 3, we introduce our SCF-SF and MC computational models. The results of calculations are summarized in section 4. Relevant experimental results are discussed in section 5, and this is followed by the Conclusions.

2. Theoretical Considerations

Theory considers a cylindrical core−shell molecular brush as an array of AB-diblock copolymer chains grafted at one (B) end onto a thin long cylinder (mimicking the main chain, or the backbone of the molecular brush) and immersed in a solvent, Figure 1. The degree of polymerization of A and B blocks of the grafted chains are n_A, $n_B \gg 1$. The spacing between the grafts h is small enough to ensure crowding of neighboring chains (number of grafted chains per unit length of the main chain, h^{-1}, characterizes the grafting density). The grafted chains are assumed to be intrinsically flexible, i.e., the Kuhn segment length is of the order of the monomer size, a. On the contrary, the main chain is assumed to be stiff on the length scale exceeding the characteristic thickness of the brush. The latter condition implies local cylindrical symmetry of the brush.

The solvent strength for A and B monomer units is characterized by monomer−monomer excluded volume parameters (second virial coefficients), $a^3\upsilon_X \cong a^3(^1/_2 - \chi_X)$, where X = A or B. Below we assume that the solvent is good for monomer units of the A blocks, $\chi_A \approx 0$, and poor for the B monomer units, $\chi_B \geq 0.5$, so that $\upsilon_B \leq 0$; $\upsilon_A \approx 1$. When $\chi_B \sim 1$, i.e., when the solvent is very poor for the B blocks, the volume fraction of monomers B in the collapsed domains approaches unity and the width of the interface between collapsed B domains and water is on the order of the monomer size $\sim a$ (strong segregation limit). Under these conditions, the A blocks can be considered as terminally attached to the surface of the B domains and the effects of interaction between A and B monomers (quantified by the corresponding Flory−Huggins parameter, $\chi_{AB} \sim 1$) are relatively weak.

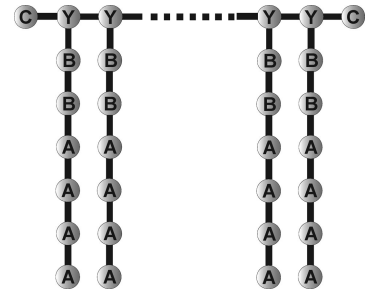

Figure 2. Model of the core−shell molecular brush C−(Y−B_{22}−A_{42})$_{192}$−C, studied in MC simulation.

We aim to rationalize (i) what the equilibrium structure adopted by the core−shell brush with collapsed B-blocks is and (ii) how the structural parameters depend on the degrees of polymerization and on the solvent strength for both A and B blocks.

There is an apparent similarity between unimolecular micelles in AB core−shell bottle-brushes and micelles formed by AB diblock copolymers in dilute solutions in selective solvents. Depending on the lengths of A and B blocks and the strength of interactions in the core and in the corona, the AB diblock copolymers assemble into equilibrium aggregates of different morphologies, i.e., spherical or cylindrical micelles, vesicles, or lamellar mesophases.

Compared to a solution of AB block copolymers, end-grafting of the copolymer chains in the core−shell molecular brush introduces additional frustration in the system. This frustration is determined by the "imposed" cylindrical symmetry of the system and by a fixed axial distance between the end-grafted copolymer chains in the brush. As a result, we expect significant differences in self-assembly behavior in solution of "free" AB diblock copolymers and in the array of identical copolymer molecules regularly grafted to the backbone of the molecular brush.

As has been shown in refs 7 and 8, the onset of collapse transition in cylindrical homopolymer brushes (which is the limiting case of the AB core−shell brush at $n_A = 0$) occurs below the Θ-point, at $|\upsilon_B| \sim n_B^{-1/3}(h/a)^{-1/3}$. The Θ-range, $|\upsilon_B| \leq n_B^{-1/3}(h/a)^{-1/3}$, where ternary repulsions dominate over binary attractions, widens upon an increase in the grafting density $(h/a)^{-1}$. At $|\upsilon_B| \gg n_B^{-1/3}(h/a)^{-1/3}$ the bottle-brush has the shape of a uniformly collapsed cylindrical globule with a polymer concentration $\sim|\upsilon_B|$ and radius $R \cong n_B^{1/2}a(h/a)^{-1/2}|\upsilon_B|^{-1/2}$. This holds as long as chains in the brush remain extended with respect to their Gaussian dimensions, i.e., $R \geq n^{1/2}a$, that is the case in the range $n_B^{-1/3}(h/a)^{-1/3} \leq |\upsilon_B| \leq (h/a)^{-1}$. Further decrease in the solvent strength down to $|\upsilon_B| \cong (h/a)^{-1}$ leads to loss of radial stretching of the chains, $R \cong n_B^{1/2}a$, and appearance of longitudinal undulations along cylindrical globule. Remarkably, within the accuracy of a scaling approach the solvent strength threshold corresponding to the instability of a uniform cylindrical shape of a collapsed brush is predicted to be independent of the degree of polymerization of grafted chains, n_B. In the

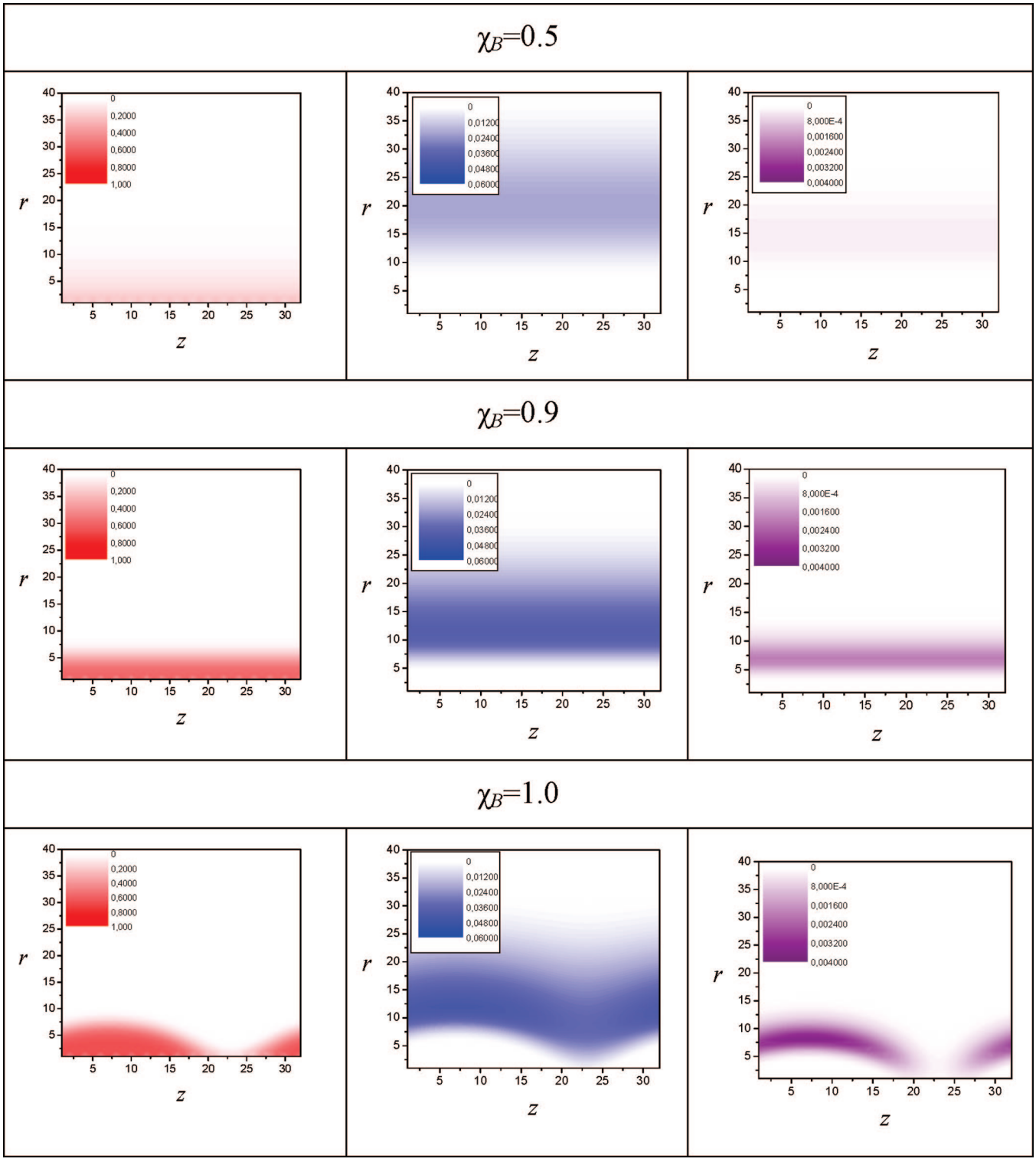

Figure 3. Concentrations of A (left) and B (middle) monomer units and A-B junction points (right) in (r, z)-coordinates obtained by SCF calculations for different values of χ_B varied from Θ- to poor solvent strength conditions. The value of $\chi_A = 0$ is constant, $\chi_{AB} = \chi_B$. The core−shell brush parameters are $n_A = n_B = 100$ and $h = 2$. Box sizes for undulated structures are optimal.

transition range, $|\upsilon_B| \approx (h/a)^{-1}$, both the characteristic wavelength and magnitude of undulations are $\sim n_B^{1/2}a$.

In the range of limiting poor solvent strength conditions, $(h/a)^{-1} < |\upsilon_B| \leq 1$, the brush loses its axial continuity and splits into quasi-spherical globular clusters comprising multiple, $p \cong n_B^{1/2}|\upsilon_B|^{1/4}(h/a)^{-3/4}$, chains. The size of collapsed core of a cluster scales as $R \cong n_B^{1/2}a|\upsilon_B|^{-1/4}(h/a)^{-1/4}$ whereas the average distance between clusters scales as $L \cong n_B^{1/2}a|\upsilon_B|^{1/4}(h/a)^{1/4}$.

The most essential feature of the transition related to longitudinal instability of uniformly collapsed cylindrical brush is that in the transition point, $|\upsilon_B| \approx (h/a)^{-1}$, the chains lose stretching in the radial direction, $R \cong n_B^{1/2}a$. In contrast, below the transition point, $|\upsilon_B| \geq (h/a)^{-1}$, the segments of the chains connecting the grafting points to the globular cores are stretched in the longitudinal direction, $L \geq n_B^{1/2}a$. A balance of conformational entropy penalty for the longitudinal stretching with

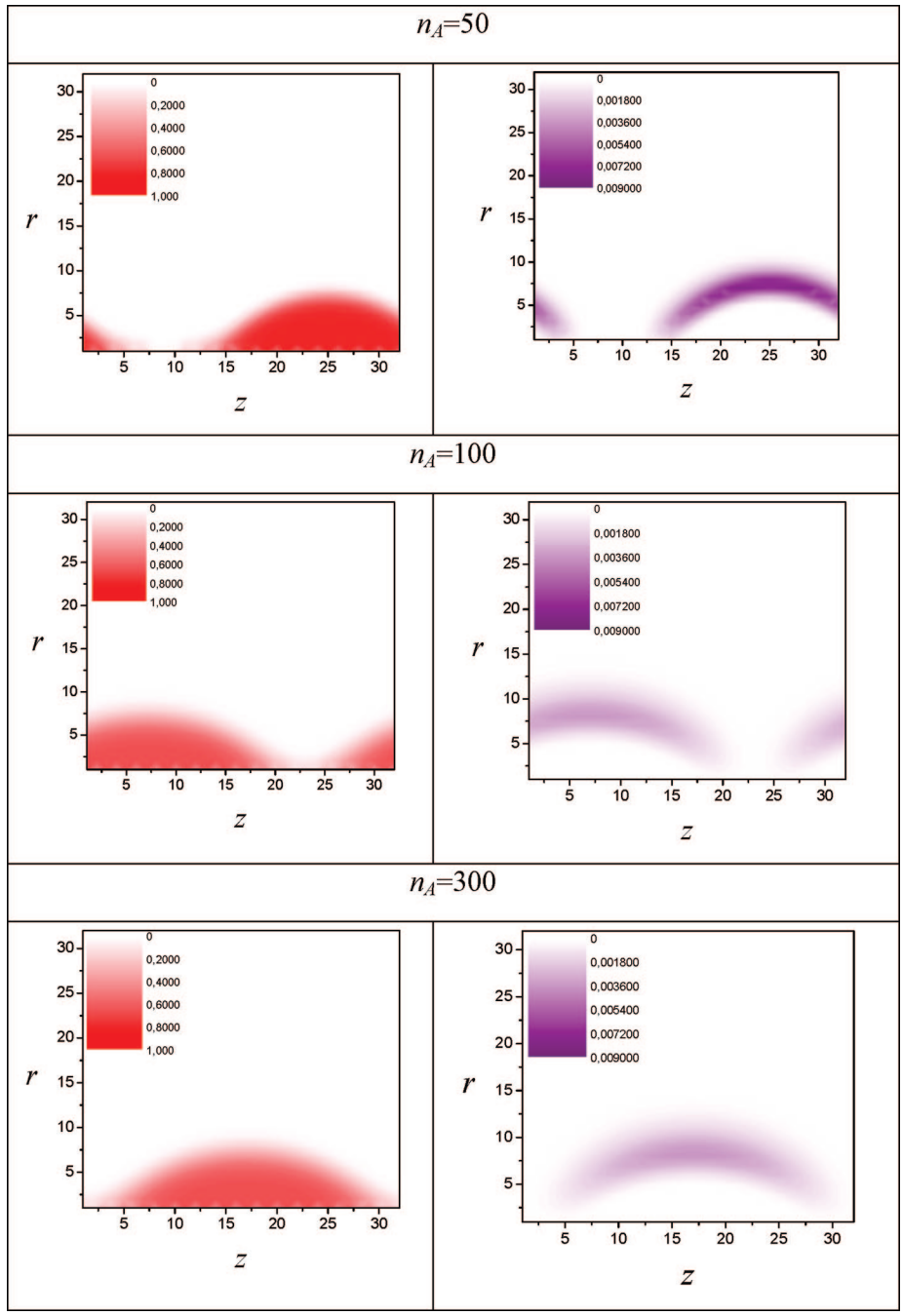

Figure 4. Concentrations of B monomer units and AB-junctions in (r, z)-coordinates obtained by SCF calculations for varied number n_A of monomer units in the A-block. $n_B = 100$, $h = 2$; the interaction parameters are set as $\chi_A = 0$, $\chi_{AB} = \chi_B = 1$.

the excess free energy of the interface of globular domains determines equilibrium number of chains comprising one domain.

We anticipate that conformational transition in core−shell molecular brush formed by strongly asymmetric, $n_B \gg n_A$, end-grafted AB-copolymer follows the same route as that in homopolymer B-brush. In particular, collapse of the core forming B-blocks into the cylindrical globule starts below the Θ-point for B homopolymer, i.e., at $|\upsilon_B| \sim n_B^{-1/3}(h/a)^{-1/3}$. The transition between cylindrical and pearl-necklace shape of the core is expected to occur at $|\upsilon_B| \approx (h/a)^{-1}$ irrespectively of the length n_B, n_A of both blocks. The transition point corresponds to vanishing of stretching of the B blocks in the radial direction and to the onset of the longitudinal stretching.

In order to rationalize the effect of the A-block on the transition and structure of the pearl-necklace intramolecular micelle in the case of arbitrary n_A, n_B, we have to keep in mind that both the thickness, $R \cong n_B^{1/2}a(h/a)^{-1/2}|\upsilon_B|^{-1/2}$, and the interfacial free energy per chain, $F_{interface}/k_BT \cong \gamma hR \cong n_B^{1/2}(h/a)^{1/2}|\upsilon_B|^{3/2}$, in the cylindrical unimolecular micelle are entirely controlled by the solvent strength, $|\upsilon_B|$, for the B-blocks of the grafted copolymer chains.

On the other hand, in the regime when B-blocks form necklace of spherical collapse domains of radius R, separated by distance L, the A blocks are attached to the surface of the B domains. On the length scale of the order of L the corona surrounding each domain retains quasi-spherical shape, whereas on larger distances from the backbone the structure of cylindrical bottle-brush formed by swollen A blocks is recovered. The free energy contribution arising from the coronal A blocks then can be presented as $F_{corona}/k_BT \cong p^{1/2} \ln(L/R) + n_A^{3/8}(h/a)^{-5/8}\upsilon_A^{1/8}$. Substituting the values of

p, L, and R presented above for the case $n_B \gg n_A$, we find that $(F_{interface} + F_{elastic})/\Delta F_{corona} \gg 1$. Hence, in scaling terms interactions between coronal A-blocks should not affect power law dependences for the size of the B-clusters and for the transition point from cylindrical to necklace unimolecular micelle structure.

3. Calculation and Experimental Methods

3.1. Self-Consistent Field (SCF) Approach. At the basis of the SCF approach is a mean-field free energy which is expressed as a functional of the volume fraction profiles (normalized concentrations) and the self-consistent field potentials. The optimization of this free energy leads for Gaussian polymer chains to the Edwards diffusion (ED) (differential) equation,[10] which for any coordinate system may be expressed as

$$\frac{\partial G(n,\mathbf{r})}{\partial n} = \frac{a^2}{6}\nabla^2 G(n,\mathbf{r}) - u(\mathbf{r})G(n,\mathbf{r}) \quad (1)$$

The self-consistent potential $u(\mathbf{r})$ represents the surroundings of a probe chain and serves as an external field used in the Boltzmann equation to find the statistical weight for each chain conformation. Consequently, the end-point distribution $G(n,\mathbf{r})$ that obeys eq 1 is related to the volume fraction profile of the polymer chains. In our case the first segments of all the grafted chains are attached to the backbone by the initial condition, and the boundary conditions provide constraints on the spatial solutions; i.e., it influences the period of the undulations.

To solve these equations rigorously, it is necessary to introduce a numerical algorithm. Such numerical scheme invariably involves space discretization (i.e., the use of a lattice). Here we follow the

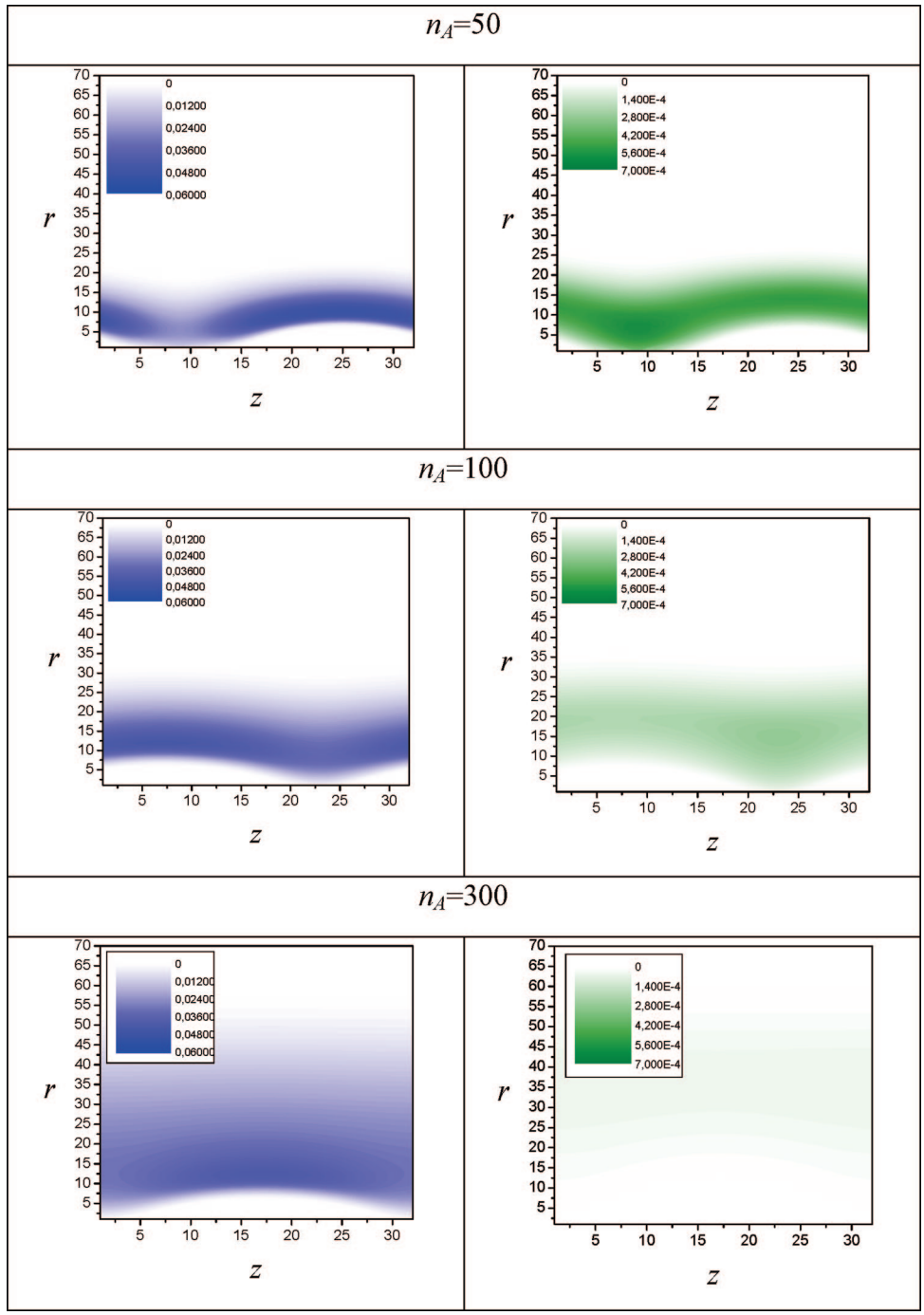

Figure 5. Concentrations of A monomer units and end-monomers of the A blocks in (r, z)-coordinates obtained by SCF calculations for varied number n_A of monomer units in the A-block. $n_B = 100$, $h = 2$; the interaction parameters are set as $\chi_A = 0$, $\chi_{AB} = \chi_B = 1$.

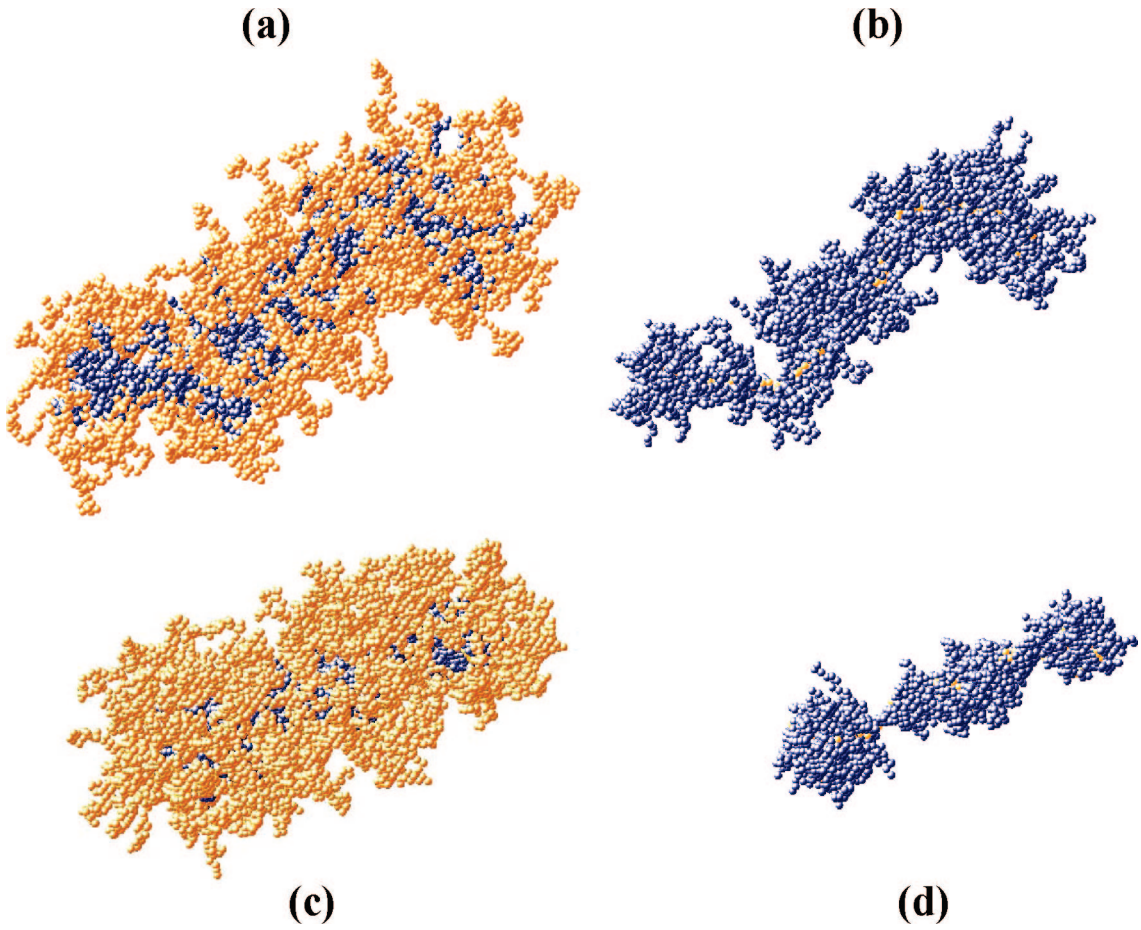

Figure 6. Snapshots of typical conformations of the molecular core−shell brush C−(Y−B_{22}−A_{42})$_{192}$−C obtained by MC simulations at infinite temperature corresponding to athermal solvent for both A and B blocks (a and b) and at finite temperature corresponding to athermal solvent for A blocks and poor solvent for B blocks (c and d). In parts a and c, all monomer units are presented, whereas in parts b and d only core-forming B monomers and the backbone Y monomers are depicted.

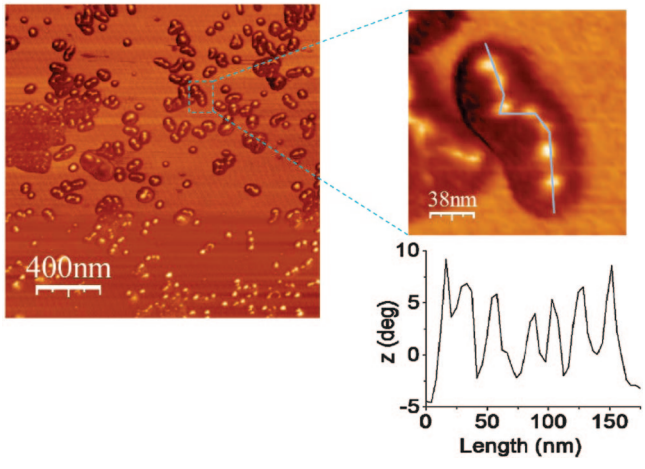

Figure 7. AFM image of core−shell cylindrical polymer brush [AA_{25}-nBA_{61}]$_{1500}$ dip-coated onto mica from toluene solution.

method of Scheutjens and Fleer (SF-SCF),[11] who used the segment size a as the cell size. A mean-field approximation is applied to a set of lattice sites. This set (often called a lattice layer) is referred to with a single coordinate **r**. The way the sites are organized in layers depends on the symmetry in the system and must be preassumed. The approach allows for, e.g., volume fraction gradients between these layers.

In order to consider a molecular bottle brush with longitudinal undulations, it is necessary to use a two-gradient version of SCF algorithm.[12] The natural geometry for this is a cylindrical coordinate system for which $\mathbf{r} = (r, z)$. In this case, all volume fraction profiles as well as other thermodynamic values depend only on the radial coordinate r and the axial coordinate z, while the mean-field approximation is used along angular coordinate.

More specifically, within our model the (rigid) main chain of a core−shell bottle-brush coincides with the axis of the cylinder (i.e., at $r = 0$). An array of polymer chains originates from this line and they are homogeneously distributed along the z-direction with an inter chain distance h between the grafting points. All chains have their first segment at a fixed z-coordinate, i.e. the chains can not slide along the line.

AB copolymer nature of the chains is taken into account via the set of Flory−Huggins parameters for monomer−solvent interactions, χ_A, χ_B, and monomer−monomer cross-interactions χ_{AB}. The solvent is assumed to be good (athermal) for A monomers, $\chi_A = 0$. The variation of the solvent strength conditions for B monomers corresponds to the variation of χ_B from 0 (good solvent conditions) to $\chi_B \sim 1$ (poor solvent conditions). In our calculations, we kept $\chi_{AB} = \chi_B$ to mimic increasing incompatibility between A and B monomers upon decrease in solubility of the B monomers.

The boundary conditions are chosen such that there is sufficient space in the radial direction to avoid system size effects. This implies that the results are obtained for the limit of very dilute solution of bottle brushes in excess of solvent. The boundary condition in the z-direction is more complicated. In principle we would like to avoid end-effects and, therefore, to consider infinitely long main chain. However we are limited to only finite box sizes in the z-direction. We use periodic boundary conditions in the z-direction to mimic an infinitely long main chain. In the limit of poor solvent conditions it is anticipated that significant gradients may occur in the z-direction (undulations). These undulations have

a particular wavelength associated to them. The boundary conditions impose a restriction to the system such that an integer number of wavelengths must fit the box size. Typically the system size in the z-direction coincides with the wavelength. The system size in the z-direction was varied in order to find the optimal wavelength of the undulations. More particularly, the free energy per chain was analyzed versus the number of chains in the simulation box for given values of the interaction parameters. Periodic minima found in the free energy were associated with the period of the equilibrium structure in the z-direction.

For convenience, we normalize all linear lengths by the cell size a. The default value for temperature used in our calculations was $T = 293$ K. There are the following parameters in our model: The dimensionless grafting density which is given by $1/h$ (instead of a/h). The numbers of monomers units are n_A, n_B, in A and B segments of the side chains. Unoccupied lattice sites are taken by a monomeric solvent (incompressible system) and the corresponding Flory−Huggins parameters for the polymer−solvent interactions are χ_A, χ_B. For convenience, we keep $\chi_A = \text{const}$ and $\chi_{AB} = \chi_B$.

3.2. Monte Carlo Simulations. The advantage of the Monte Carlo method is the ability to visualize conformational changes directly without assuming cylindrical symmetry. The model employed here is a coarse-grained lattice polymer model on a simple cubic lattice. To be specific, the method is a simple extension of the bead-and-bond lattice polymer MC method called the "diagonal bond method": A bead occupies only one lattice point to ensure excluded volume interactions as usual. The difference is that the bond length can be 1, $\sqrt{2}$, or $\sqrt{3}$ in the unit of lattice spacing.[13] We consider 26 bond directions (6 nearest neighbors, 12 second nearest neighbors, and 8 third nearest neighbors), and thus the chain is very flexible. It should be noticed that monomers do not correspond to real monomers but to Kuhn segments.

Here we take cylindrical core−shell brush $C-(Y-B_{22}-A_{42})_{192}-C$ in a solvent, where B is a solvophobic inner (core) monomer, A is a solvophilic outer (shell) monomer, Y is the main chain monomer (a junction point), and C is an end point of a backbone polymer. See the model depicted in Figure 2. Vacant sites act as solvent S. To mimic solovophobicity, contact energies $E_{\alpha\beta}$ are considered when the distance is within the body diagonal distance in the unit of lattice spacing. Here $E_{\alpha\alpha} = 0$, $E_{\alpha\beta} > 0$ when $\alpha \neq \beta$, where α,β = A, B, C, Y, S.

$$E_{AB} = E_{SB} = 1; \quad E_{BC} = E_{CA} = E_{YA} = E_{YB} = E_{YC} = E_{SA} = E_{SY} = E_{SC} = 0 \quad (2)$$

The total energy is described by $E = \Sigma_{i \neq j} E_{\alpha_i\alpha_j}$, where summation runs over neighboring lattice sites. Since the number of neighbors is 24, if two linked monomers are excluded, the Flory−Huggins parameter is estimated by

$$\chi_{\alpha\beta} = \frac{24E_{\alpha\beta}}{k_B T} = 24\beta E_{\alpha\beta} \quad (3)$$

where k_B is the Boltzman constant, T is the absolute temperature, and β is the inverse temperature defined by $\beta = 1/k_B T$. The MC procedure is the following: We select one bead randomly and choose a trial move randomly out of possible moves: If the trial site is a vacancy, we determine to move or not to move according to the Metropolis algorithm. The transition probability to the trial state is $\min[1, \exp(-\beta\Delta E)]$, where $\Delta E = E_{trial} - E$, and E_{trial} and E are energies corresponding to the trial and the present state, respectively, and then start from the first; namely, we choose the next bead randomly again. If the trial is not a vacancy, we start from the first. The system is prepared as totally randomized at the infinite temperature, and then we adopt slow cooling processes to avoid being caught in quasi-stable states.

3.3. Synthesis and Characterization of Core−Shell Brushes. A core−shell cylindrical brush with poly(acrylic acid) (PAA) core and poly(*n*-butyl acrylate) (PnBA) shell $[AA_{25}\text{-}nBA_{61}]_{1500}$ was prepared by the combination of anionic polymerization and atom transfer radical polymerization (ATRP), which is described in detail in our previous work.[14] Here, this polymer has a backbone with DP = 1500 and side chains with 25 AA units forming the core and 61 nBA units forming the shell. The core−shell cylindrical brush $[MAA_{60}\text{-}OEGMA_{200}]_{1500}$ with 60 units of methacrylic acid (MAA) as the core and 200 units of oligo(ethylene glycol methacrylate) (OEGMA) as the shell was prepared in a similar manner.

Atomic force microscopy (AFM) measurements were performed on a Digital Instruments Dimension 3100 microscope operated in tapping mode. The microcantilever used for the AFM measurements were from Olympus with resonant frequency between 284.3 and 386.0 kHz, and spring constant ranging from 35.9 to 92.0 N/m. The sample were prepared by diluting 0.1 mL of 1 g/L $[AA_{25}\text{-}nBA_{61}]_{1500}$ solution (in chloroform/methanol l/1 by volume mixed solvent) into 10 mL of toluene. Then the sample was dip-coated onto a freshly cleaved mica surface.

Cryo-TEM measurements were performed on a Zeiss EM922 EFTEM with an acceleration voltage of 200kV. The concentrations of brush $[MAA_{60}\text{-}OEGMA_{200}]_{1500}$ in water solution was ca. 0.01 g/L.

4. Results of Modeling and Discussion

4.1. SCF Modeling. We start with discussing results of the SCF modeling, corresponding to molecular brushes with sufficiently stiff backbone. These brushes retain cylindrically symmetric configuration on the length scale significantly exceeding the axial distance between neighboring grafted chains.

In Figure 3, the monomer density profiles for A and B monomer units and for the junction points (terminal monomer unit in the B-block) are presented in (r, z) coordinates for several values of χ_B corresponding to variation of the solvent strength for the B block from Θ to poor solvent conditions. The copolymer composition is symmetric, $n_A = n_B = 100$ and grafting density is $1/h = 0.5$. One can see that an increase in χ_B from 0.5 to 0.9 leads to the progressive collapse of the B blocks and appearance of a unimolecular micelles with a core of uniform cylindrical shape and with the bottle-brush-like corona formed by swollen A blocks. The end-segments of the B blocks get progressively localized at the interface of the collapsed cylindrical core. Remarkably, homologous diblock AB copolymers form under the same conditions only spherical starlike micelles. However, upon further increase in χ_B, homogeneous in z-directions cylindrical core of the unimolecular micelle splits into separated clusters with well-defined size and shape.

More detailed analysis in the interval $0.9 < \chi < 1$ allowed us to localize the transition point $\chi_{tr} \approx 0.97$. Moreover, our analysis indicates that an increase in the number of monomers both in A and B blocks leads to very weak increase in χ_{tr} (up to 1.06). This finding is in a good agreement with predicted by scaling approach absence of power law dependence of χ_{tr} on the number of monomers in a grafted chain.

Note that the use of periodic boundary conditions in z-direction leads to two following consequences for the undulated structures: (1) an integer number of clusters is always obtained for any (sufficiently large) box size, and (2) the placement of the structure in the box is not necessarily symmetric in the z-direction with respect to the center of the box.

Since the box size remains unchanged in each run of the SCF method, for each set of parameters a series of calculation for different box sizes in the z-direction was done to determine the optimal box size and, hence, the structure's period corresponding to the minimum of the free energy per side chain as a function of the box size.

Consider now the influence of the length of the corona chains on the parameter of the pearl-necklace structure. Figures 4 and 5 presents the density plots for A, and B monomer units and A and B terminal monomers (the latter can be considered as the

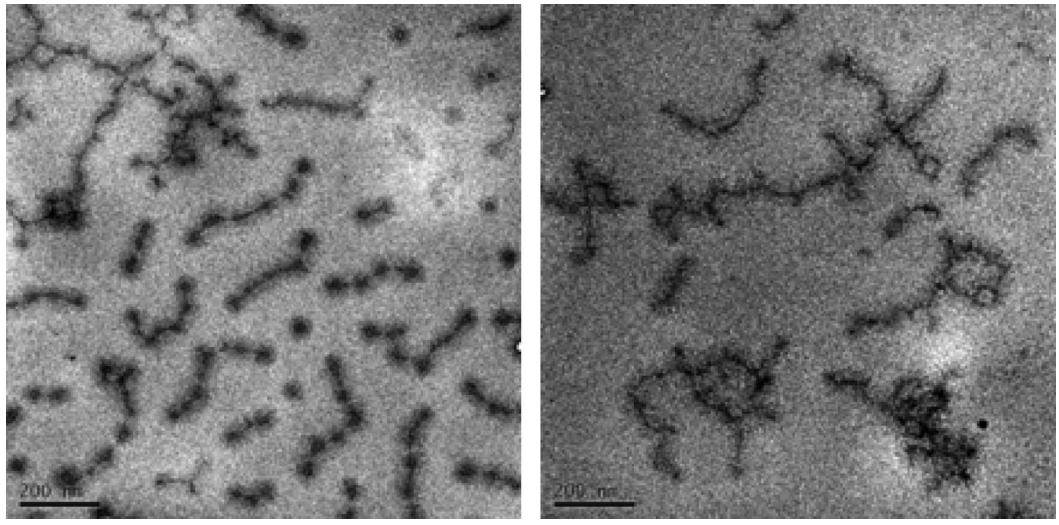

Figure 8. Cryo-TEM image of core−shell polymer brush $[MAA_{60}OEGMA_{200}]_{1500}$ in water at pH = 4 (left) and pH = 7 (right).

A-B junction points) From these profiles one can see that in the given range of n_A variation (from 50 to 300) there is no change in the structure period and almost no change in the shape of the collapsed core. However, with the increase in n_A, we can observe smearing of the A/B interface and the delocalization of the A−B junction points. This effect is obvious and caused by the stretching force exerted by swollen and crowded coronal chains. Note that for the B density plots in Figure 4 the same scale on r and z axes is set, so they give true shape of the core "pearls" (micelles) in the undulated structure.

Looking at the corona profiles at $n_A = 300$ in Figure 5 we notice that in this case the profile can be divided into two parts: close to the A/B interface, the A chains are stretched as in the spherical brush (effective area per chain $\sim r^2$) whereas far from the interface they do not "feel" the core and behave as in the cylindrical bottle-brush (effective area per chain $\sim r$).

We remind the reader, that the imposed cylindrical symmetry of the molecular brush and fixed axial separation between the grafting points is an essential ingredient of the employed SCF analysis scheme. Physically this situation corresponds either to molecular brushes with sufficiently rigid backbone (with the Kuhn segment length exceeding the thickness of the brush) or to a core−shell brush with long A blocks. In the latter case, strong repulsion between crowded solvophilic A blocks keeps the brush in a locally cylindrically symmetrical configuration.

4.2. MC Simulations. In contrast to the SCF approach, the Monte-Carlo simulations explicitly account for the flexibility of the backbone of the molecular brush. As was discussed in ref 9, flexibility of the main chain allows reducing the axial distance between grafting points upon collapse of the molecular bottle brush in poor solvent and stabilizes locally cylindrical configuration.

Figure 6 presents typical snapshots of the conformation of the core−shell brush obtained in MC simulations for the cases when the solvent is equally good for both core and shell blocks (Figure 6a,b) and under conditions of poor solvent for the core-forming B blocks (Figure 6c,d). In the latter case one clearly observes the formation of multiple collapsed B domains stabilized by repulsion between swollen A shells ("pearl-necklace" structure). Remarkably, the total length of the molecular brush is weakly affected by the conformational changes in the core-forming block, as it is controlled by repulsion between the shell-forming A blocks.

5. Experimental Observations

We had already observed earlier that cylindrical core−shell brushes with PAA core and PnBA corona show a pearl necklace structure, when Cd^{2+} or Fe^{3+} ions form a polychelate with the PAA core.[2,3] According to the predictions above, this is due to the poor solubility of the PAA-ion complexes. Thus, we undertook a study of those polymers in a poor solvent for PAA, toluene. Figure 7 shows an atomic force microscopy (AFM) image after dip-coating onto mica. The pearl-necklace structure is clearly observed.

Figure 8 shows a cryogenic transmission electron micrograph (cryo-TEM) of a brush with a core poly(methacrylic acid) (PMAA) and a poly(oligoethyleneglycol methacrylate) (POEGMA) corona (DP of oligo(ethylene glycol) $\sim$ 5) in water. At pH = 7, the typical cylindrical structure of polymer brushes is observed. However, at pH = 4 the PMAA collapses, again showing the pearl-necklace structure.

6. Conclusions

Both the experimental evidence and the results of our SCF and MC modeling provide unambiguous evidence that unimolecular cylindrical micelles formed in core−shell molecular brushes with collapsed inner blocks are stable within a limited range of conditions, but they exhibit instability with respect to longitudinal undulations and intramolecular nanostructuring upon a decrease in the solvent strength for the collapsed inner block.

Remarkably, unimolecular cylindrical micelles in core−shell molecular brushes with sufficiently rigid backbone may exist even under conditions when homologous diblock copolymers form only spherical micelles in the solution.[15,16] The physical origin of the instability of a unimolecular cylindrical micelle is a balance of the excess free energy of the interface between the collapsed domains and the poor solvent and the conformational entropy of the B blocks stretched either in radial or in longitudinal direction. Therefore, both the transition point and structural properties (aggregation number, longitudinal period, etc.) of the intramolecular collapsed nanodomains are determined primarily by the degree of polymerization and solvent quality for the solvophobic B block. For molecular brushes with a stiff (or semiflexible) main chain the effect of the solvophilic A block on nanostructures formed by the solvophobic B blocks is found to be of marginal importance.

An experimental evidence of the appearance of the necklace unimolecular micelles either because of low solubility of the

core-forming block in the selective solvent or due to formation of insoluble complexes with multivalent ions proves quite a general character of this behavior for molecular core−shell brushes.

Acknowledgment. This work has been performed as a part of the collaborative research project SONS-AMPHI within the European Science Foundation EUROCORES Program, and has been partially supported by funds from the EC Sixth Framework Program through the Marie Curie Research and Training Network POLYAMPHI. Support by the German Science Foundation (DFG, Projects Mu896/22 and SFB 481/B9), the Dutch National Science Foundation (NOW) and the Russian Foundation for Basic Research (RFBR) through Joint Project 047.017.026/06.04.89402 and Project 05.03.33126 is gratefully acknowledged.

Supporting Information Available: Movie (.mov) of the Monte Carlo simulations of cylindrical core−shell brush $C-(Y-B_{22}-A_{42})_{128}-C$ performed at different solvent strength conditions for the core-forming B-blocks. This material is available free of charge via the Internet at http://pubs.acs.org.

References and Notes

(1) (a) Tsukahara, Y.; Mizuno, K.; Segawa, A.; Yamashita, Y. *Macromolecules* **1989**, *22*, 1546–1552. (b) Dziezok, P.; Sheiko, S. S.; Fischer, K.; Schmidt, M.; Möller, M. *Angew. Chem. Int. Ed* **1997**, *36*, 2812–2815. (c) Bolisetty, S.; Airaud, C.; Xu, Y.; Müller, A. H. E.; Harnau, L.; Rosenfeldt, S.; Lindner, P.; Ballauff, M. *Phys. Rev. E* **2007**, *75*, 040803. (d) Pakula, T.; Zhang, Y.; Matyjaszewski, K.; Lee, H.-i.; Börner, H.; Qin, S.; Berry, G. C. *Polymer* **2006**, *47*, 7198–7206. (e) Zhang, B.; Grohn, F.; Pedersen, J. S.; Fischer, K.; Schmidt, M. *Macromolecules* **2006**, *39*, 8440. (f) Rathgeber, S.; Pakula, T.; Wilk, A.; Matyjaszewski, K.; Beers, K. *J. Chem. Phys.* **2005**, *122*, 124904: For a review, see:(g) Zhang, M.; Müller, A. H. E. *J. Polym. Sci., Part A: Polym. Chem.* **2005**, *43*, 3461–3481.

(2) Zhang, M.; Drechsler, M.; Müller, A. H. E. *Chem. Mater.* **2004**, *16*, 537–543.

(3) Zhang, M.; Estournés, C.; Biestch, W.; Müller, A. H. E. *Adv. Funct. Mater.* **2004**, *14*, 871–882.

(4) Birshtein, T. M.; Zhulina, E. B. *Polym. Sci. USSR* **1985**, *27*, 570–581.

(5) Birshtein, T. M.; Borisov, O. V.; Zhulina, E. B.; Khokhlov, A. R.; Yurasova, T. A. *Polym. Sci. USSR* **1987**, *29*, 1293–1300.

(6) Fredrickson, G. *Macromolecules* **1993**, *26*, 2825–2831.

(7) Borisov, O. V.; Zhulina, E. B.; Birshtein, T. M. *Polym. Sci. USSR* **1988**, *30*, 772–779.

(8) Zhulina, E. B.; Borisov, O. V.; Pryamitsyn, V. A.; Birshtein, T. M. *Macromolecules* **1991**, *24*, 140–149.

(9) Sheiko, S. S.; Borisov, O. V.; Prokhorova, S. A.; Möller, M. *Eur. Phys. J. E* **2004**, *13*, 125–131.

(10) de Gennes, P. G. *Scaling Concepts in Polymer Physics*; Cornell University Press: Ithaca, NY, and London, 1979.

(11) Fleer, G. J.; Cohen Stuart, M. A.; Scheutjens, J. M. H. M.; Cosgrove, T.; Vincent, B. *Polymers at Interfaces*; Chapman and Hall: London, 1993.

(12) Feuz, L.; Leermakers, F. A. M.; Textor, M.; Borisov, O. V. *Macromolecules* **2005**, *38*, 8891–8901.

(13) Dotera, T.; Hatano, A. *J. Chem. Phys* **1996**, *105*, 8413–8427.

(14) Zhang, M.; Breiner, T.; Mori, H.; Müller, A. H. E. *Polymer* **2003**, *44*, 1449–1458.

(15) Borisov, O. V.; Zhulina, E. B. *Macromolecules* **2003**, *36*, 10029.

(16) Zhulina, E. B.; Adam, M.; Sheiko, S.; LaRue, I.; Rubinstein, M. *Macromolecules* **2005**, *38*, 5330.

MA800125Q